Journal of Hazardous Materials 165 (2009) 100–110

Contents lists available at ScienceDirect

Journal of Hazardous Materials

journal homepage: www.elsevier.com/locate/jhazmat

Removal of Direct N Blue-106 from artificial textile dye effluent using activated carbon from orange peel: Adsorption isotherm and kinetic studies

Azza Khaled, Ahmed El Nemr*, Amany El-Sikaily, Ola Abdelwahab

Department of Pollution, Environmental Division, National Institute of Oceanography and Fisheries, El-Anfoushy, Kayet Bey, Alexandria, Egypt

ARTICLE INFO

Article history:
Received 25 January 2007
Received in revised form 9 June 2008
Accepted 23 September 2008
Available online 11 October 2008

Keywords:
Orange peel
Activated carbon
Kinetics
Isotherm
Direct N Blue-106
Adsorption
Wastewater

ABSTRACT

The purpose of this study is to suggest an efficient process, which does not require a huge investment for the removal of direct dye from wastewater. Activated carbon developed from agricultural waste material was characterized and utilized for the removal of Direct Navy Blue 106 (DNB-106) from wastewater. Systematic studies on DNB-106 adsorption equilibrium and kinetics by low-cost activated carbons were carried out. Adsorption studies were carried out at different initial concentrations of DNB-106 (50, 75, 100, 125 and 150 mg l^{-1}), contact time (5–180 min), pH (2.0, 3.0, 4.7, 6.3, 7.2, 8.0, 10.3 and 12.7) and sorbent doses (2.0, 4.0 and 6.0 g l^{-1}). Both Langmuir and Freundlich models fitted the adsorption data quite reasonably ($R^2 > 97$). The maximum adsorption capacity was 107.53 mg g^{-1} for 150 mg l^{-1} of DNB-106 concentration and 2 g l^{-1} carbon concentration. Various mechanisms were established for DNB-106 adsorption on developed adsorbents. The kinetic studies were conducted to delineate the effect of initial dye concentration, contact time and solid to liquid concentration. The developed carbon might be successfully used for the removal of DNB-106 from liquid industrial wastes.

1. Introduction

Treatment of the effluent from the dyeing and finishing processes in the textile industry is one of the most significant environmental problems. Since most synthetic dyes have complex aromatic molecular structures which make them inert and biodegradable difficult when discharged into the environment. Colored wastes are harmful to aquatic life in rivers, lakes and Sea where they are discharged [1,2]. Colored water hinders light penetration and may in consequence disturb biological processes in water-bodies. Moreover, dyes itself are highly toxic to some organisms and hence disturb the ecosystem [3,4]. Dyes can cause allergic dermatitis, skin irritation, cancer, mutation, etc. In addition, biodegradation of some of them produce aromatic amines, which are highly carcinogenic [5,6]. The continuous exposure of workers in the textile industries is linked to a higher bladder cancer risk [7]. In addition, a linked between breast cancer and the use of hair coloring products have also been reported [8].

Dyes are usually stable to photo-degradation, bio-degradation and oxidizing agents [9], which led to intensive investigations on physical or chemical methods to remove color from textile effluent. These studies include the use of coagulants [10], ultra-filtration [11] and electro-chemical [12,13]. In addition to adsorption methods, which are the most widely used techniques [14–18]. The advantages and disadvantages of each technique have been extensively reviewed [19]. Of these methods, adsorption has been found to be an efficient and economic process to remove dyes, pigments and other colorants and also to control the bio-chemical oxygen demand [19].

Recently, various kinds of activated carbon have been achieved from different agriculture wastes and used as low-cost adsorbents for removal of heavy metals, organics and dyes from aqueous solution. Activated carbon has many applications, one of which is removal of hazard materials from water, air and many chemical and natural products [20,21].

In our laboratory, the work is in progress to develop activated carbons from agriculture wastes such as, rice husk, sawdust, corn cob, orange peel, etc. and evaluate its capability to remove hazard materials from water. This study was to evaluate the possibility of using activated carbon developed from dried orange peel to remove Direct Navy Blue-106 (DNB-106). Dried orange peel was previously investigated to adsorb acid violet 17 [22] and Direct Red 23 and 80 [23,24]. Systematic evaluation of the parameters involved, such as pH, sorbents mass, initial dye concentration and time. The interference of the simulated wastewater on the adsorption of Direct Navy Blue-106 was additionally investigated.

* Corresponding author. Tel.: +20 35740944; fax: +20 35740944.
E-mail address: ahmedmoustafaelnemr@yahoo.com (A.E. Nemr).

0304-3894/$ – see front matter © 2008 Elsevier B.V. All rights reserved.
doi:10.1016/j.jhazmat.2008.09.122

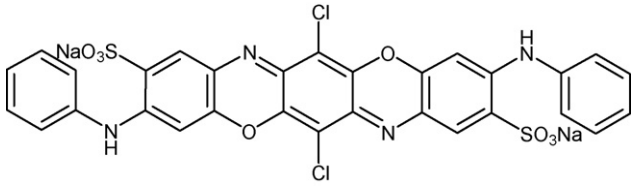

Fig. 1. Chemical structure of DNB-106 {6,13-dichloro-3,10-bis-phenylamino-benzo[5,6][1,4]oxazino[2,3-b]phenoxazine-2,9-disulfonic acid}, CI 51300.

2. Materials and methods

2.1. Biomass

Orange peel was collected from a local fruit field in the north of Egypt and washed with tap water followed by washing with distilled water and oven dried at 105 °C for 4 days followed by milled, sieved and the particles ≤0.500 mm was selected for use.

2.2. Activated carbon from orange peel (COP)

The dried orange peel biomass 2.0 kg was added in small portion to 2.0 l of 98% H_2SO_4 during 10 h and the resulting reaction mixture was kept for 2 days at room temperature followed by refluxing for 6 h in fume hood. Cool in ice bath and the reaction mixture was poured onto cold water (5 l) and filtered. The obtained dehydrated orange peel was heated in an open oven at 120 °C for 24 h followed by immersed in 5% $NaHCO_3$ (3.0 l) overnight to remove any remaining acid. The obtained carbon was then washed with distilled water until pH of the activated carbon reached 6, dried in an oven at 150 °C for 48 h in the absence of oxygen and sieved to the particle size ≤0.200 mm and kept in a glass bottle until used.

2.3. Preparation of synthetic solution

A stock solution of 1000 mg l^{-1} was prepared by dissolving the appropriate amount of Direct Navy Blue-106 (DNB-106; 92%; molecular formula is $C_{30}H_{16}Cl_2N_4Na_2O_8S_2$; MWt = 741.49; CI 51300, obtained from ISMA Dye Company, Kafr-El-Dawar, Egypt) in 500 ml and completed to 1000 ml with distilled water. Fig. 1 displays the chemical structure of the DNB-106. Concentrations ranged between 5 and 150 mg l^{-1} were prepared from the stock solution to have the stander curve (Fig. 2). All the chemicals used throughout this study were of analytical-grade reagents. Double-distilled water was used for preparing all of the solutions and reagents. The initial pH is adjusted with 0.1 M HCl or 0.1 M NaOH. All the adsorption experiments were carried out at room temperature (27 ± 2 °C).

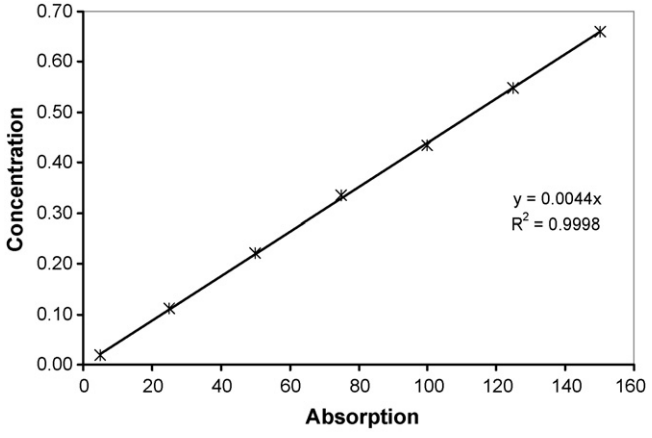

Fig. 2. Standard curve of Direct Navy Blue-106 using concentration range from 5 to 150 mg l^{-1} at room temperature.

2.4. Preparation of simulated dye wastewater

The simulated wastewater of DNB-106 was prepared by dissolving of 40 mg of NaCl and 40 mg of Na_2SO_4 crystal in 1000 ml of 150 mg l^{-1} of DNB-106. The obtained solution was used instead of the above-prepared solution in distilled water.

2.5. Batch biosorption studies

2.5.1. Effect of pH on DNB-106 biosorption

To study the effect of pH on the DNB-106 adsorption using COP, the experiments were carried out at 75 mg l^{-1} initial dye concentration with 0.6 g/100 ml COP mass at 27 ± 2 °C for 3 h equilibrium time. The initial pH values were adjusted to 1, 2, 3, 3.9, 4.7, 6.3, 7.2, 7.9, 10.3 and 12.8 with 0.1 M HCl or 0.1 M NaOH using pH meter (Check: mate 90, Corning, NY). The suspensions were shaken using agitation speed (200 rpm) for 3 h and the amount of DNB-106 adsorbed determined by abstracting (after centrifugation using centrifuge). The effect of pH adjustment at different values on the chemistry of dye was checked and it has no effect on the absorbance or wavelength.

2.5.2. Effect of COP dose

The effect of sorbents dose on the equilibrium uptake of DNB-106 (50, 75, 100, 125 and 150 mg l^{-1} dye concentration) was investigated with COP concentrations of 2, 4, 6, 8 and 10 g l^{-1} at pH 2. The experiments were performed by shaking known DNB-106 concentration with the above different COP concentrations to the equilibrium uptake (3 h) and the amount of DNB-106 adsorbed determined.

2.5.3. Kinetics studies

Sorption studies were conducted in 300 ml conical flasks at solution pH 2.0. COP (2, 4, 6 g l^{-1}) was mixed individually with 100 ml of DNB-106 solution (50, 75, 100, 125, 150 mg l^{-1}) and the suspensions were shaken at room temperature (27 ± 2 °C). Samples of 1.0 ml were collected from the duplicate flasks at required time intervals, viz. 5, 10, 20, 30, 45, 60, 90, 120, 150 and 180 min and were centrifuged for 5 min. The clear solutions were analyzed for residual DNB-106 concentration in the solution.

2.5.4. Adsorption isotherm

Batch sorption experiments were carried out in 300 ml conical flasks at room temperature on a shaker for 3 h. The COP (0.2, 0.4 and 0.6 g) was thoroughly mixed with 100 ml of DNB-106 aqueous solutions. The isotherm studies were performed by varying the initial DNB-106 concentrations from 50 to 150 mg l^{-1} at pH 2.0, which was adjusted using 0.1 M HCl or 0.1 M NaOH before addition of COP and maintained throughout the experiment. After shaking the flasks for 3 h, the reaction mixture was analyzed for the residual DNB-106 concentration.

The concentration of DNB-106 in solution was measured by using a direct UV–vis spectrophotometric method using UV–vis spectrophotometer (Milton Roy, Spectronic 21D) using silica cells of path length 1 cm at wavelength λ 660 nm, and DNB-106 concentration was determined by comparing absorbance to a calibration curve mentioned above. All the experiments are duplicated and only the mean values are reported. The maximum deviation observed was less than ±5%.

Adsorption of DNB-106 from simulated wastewater was studied using 6 g l^{-1} of COP and DNB-106 concentrations 150 mg l^{-1} at ini-

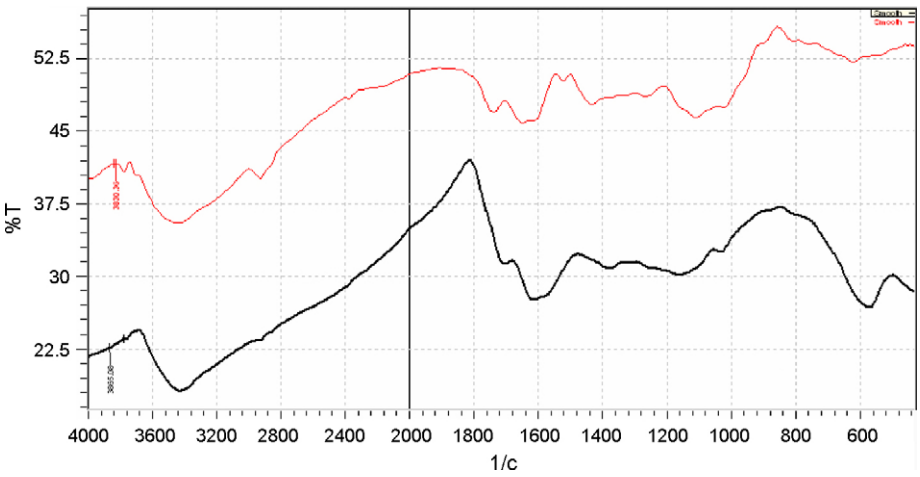

Fig. 3. The upper curve is for orange peel (OP) and the bottom curve is for carbon orange peel (COP).

tial pH 2.0. The amount of dye adsorbed onto carbon, q_e (mg g^{-1}), was calculated by the following mass balance relationship:

$$q_e = (C_0 - C_e) \times \frac{V}{W} \quad (1)$$

where C_0 and C_e are the initial and equilibrium liquid-phase concentrations of DNB-106, respectively (mg l^{-1}), V the volume of the solution (l), and W is the weight of the COP used (g).

3. Results and discussion

3.1. FTIR analysis

To determine which functional groups were responsible for metal uptake, an FTIR analysis for orange peel carbon (OPC) and orange peel (OP) was performed using KBr disk (Fig. 3). The spectra display a number of adsorption peaks, indicating the complex nature of the material examined. FTIR of the orange peel showed broad intense absorption peaks around 3429 cm^{-1} which is indicative of the existence of bonded hydroxyl groups and the peak observed at 2760 cm^{-1} can be assigned to the C–H group. The peak observed at 1703 is due to CO and the peak at 1612 cm^{-1} is due to the C=C stretching that can be attributed to the aromatic C–C bond. The peaks around 1420 cm^{-1} are due to the symmetric bending of CH_3 and the peaks at 1280 cm^{-1} C–O stretching of COOH or indicate the presences of $-SO_3$. FTIR spectrum of OPC (Fig. 3) shows a band around 3480 cm^{-1} which assigned to OH stretching vibration and its peak intensity is lower than that of FTIR of non-carbonized plant material; this finding is apparently due to the fact that H_2SO_4 initiated bond cleavage, leading to dehydration and elimination reactions that release volatile substances. H_2SO_4 breaks many bonds in aliphatic and aromatic species present in the precursor material leading to liberation and elimination of many light and volatile substances causing partial aromatization and thus carbonization. The weak bands at 3835 cm^{-1} was assigned to aliphatic groups stretching vibration. Also, the band at 1620 cm^{-1} assigned to C=C skeletal stretching in condensed aromatic system. These indicate that carbonization of orange peel leads to increase aromaticity, decomposition and cracking of a great number of structures. From view of sulfur-related absorption bands, it is seen that new absorption bands appeared in the spectrum of activated carbon sample at 1383 and 580 cm^{-1} assigned to asymmetric and symmetric stretching vibration of SO_2 and symmetric stretching vibration of S–O groups confirming the presence of surface SO_2 complex. The IR spectra of orange peel and its activated carbon shown that sulfate group may involve in the binding of pollutant.

3.2. Effect of system pH on DNB-106 uptake

The pH of the system is very effective on the adsorption capacity of adsorbate molecule presumably due to its influence on the surface properties of the adsorbent and ionization/dissociation of the adsorbate molecule. However, two possible mechanisms of adsorption of dyes on COP adsorbent may be considered: (a) electrostatic interaction between the adsorbent and dye and (b) the chemical reaction between the dye and the adsorbent. Fig. 4 shows the effect of pH on the removal of DNB-106 from aqueous solution. When initial pH of the dye solution was increased from 2 to 3, the percentage removal decreased from 93.5 to 72.5%. With increase in pH from 3 to 4, the percent removal decreased from 72.5 to 45%. With further increased in pH to 7.2 there was a slight decrease in percent removal from 45 to 35.9, while increase of the pH value from 7.2 to 12.75 led to slight increase in percent removal from 35.9 to 43.5%. Lower adsorption of DNB-106, an anionic dye, at alkaline pH is provable due to the presence of excess of OH^- ions competing with the dye anions for the adsorption sites. At the acidic pH, the number of positively charged sites increase which favors the adsorption of the anions due to electrostatic attraction. The lowest adsorption occurred at pH 7.2 and the greatest adsorption occurred at pH ~ 2.0. Moreover, the decreasing in the adsorption of DNB-106

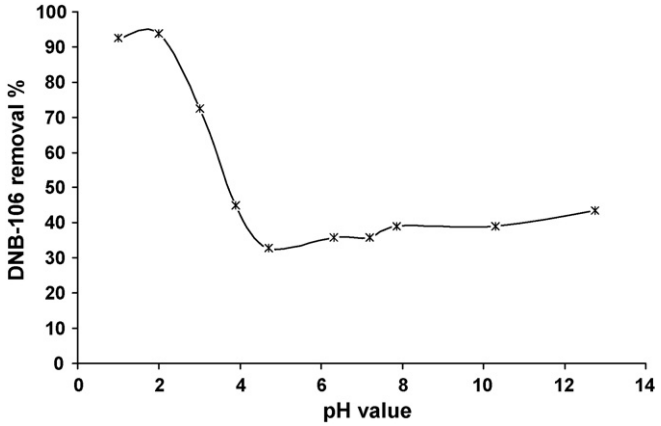

Fig. 4. Effect of system pH on adsorption of DNB-106 (100 mg l^{-1}) onto COP (0.6 g/100 ml) at 27 ± 2 °C.

with increasing of pH value is also due to the competition between anionic dye and excess OH^- ions in the solution which may be due to the fact that the high concentration and high mobility OH^- ions are preferentially adsorbed compared to dye anions. A negatively charged surface site on the COP dose not favors the adsorption of anionic DNB-106 molecules due to the electrostatic repulsion. Similar trend of pH effect was observed for the adsorption of Direct Red 28 and Acid Violet on activated carbon prepared from coir pith [25,26], as well as for the adsorption of Direct Blue 2B and Direct Green B on activated carbon prepared from Mahogany sawdust [27]. That may be attributed to the hydrophobic nature of the developed carbon which led to absorbing hydrogen onto the surface of the carbon when immersed in water and make it positively charged. At pH value >7.2 a small coagulated mass of DNB-106 was observed, which explain the small increase in the dye removal at pH 12.75.

3.3. Effect of contact time

The relation between adsorption of DNB-106 and contact time were investigated to identify the rate of dye removal. Fig. 5 shows the percentage removal of DNB-106 at different initial dye concentrations ranging from 50 to 150 mg l^{-1} and pH 2.0. The adsorption increases with increasing contact time. It was found that more than 70% removal of dye concentration occurred in the first 10 min, and thereafter the rate of adsorption was found to be slow. The rapid adsorption at the initial contact time is due to the availability of the positively charged surface of adsorbent which led to fast electrostatic adsorption of the anionic DNB-106 from the solution at pH 2.0. The later slow rate of dye adsorption is probably occurred due to the electrostatic repulsion between the adsorbed negatively charged sorbate species onto the surface of adsorbent and the available anionic sorbate species in solution as well as the slow pore diffusion of the solute ion into the bulk of the adsorbent. The equilibrium was found to be nearly 3 h when the maximum dye adsorption capacity was reached.

3.4. Effect of initial DNB-106 concentration

The experimental results of the sorption of DNB-106 on COP at various initial dye concentrations are shown in Fig. 6. The experiments were carried out at three adsorbent doses (0.2, 0.4 and 0.6 g/100 ml) in the test solution, room temperature ($27 \pm 2\,^{\circ}C$), pH 2.0 and at different initial concentrations of DNB-106 (50, 75, 100, 125 and 150 mg l^{-1}) for 3 h. The sorption capacities at equilibrium, q_e, increased from 20.42 to 54.39, 11.36 to 28.34 and 7.99

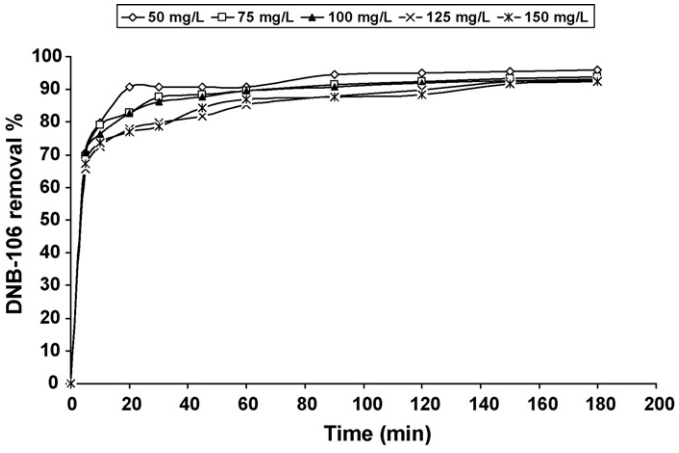

Fig. 5. Effect of contact time on the removal of different initial concentrations of DNB-106 (50, 75, 100, 125 and 150 mg l^{-1}) using COP (0.6 g/100 ml) at pH 2.0.

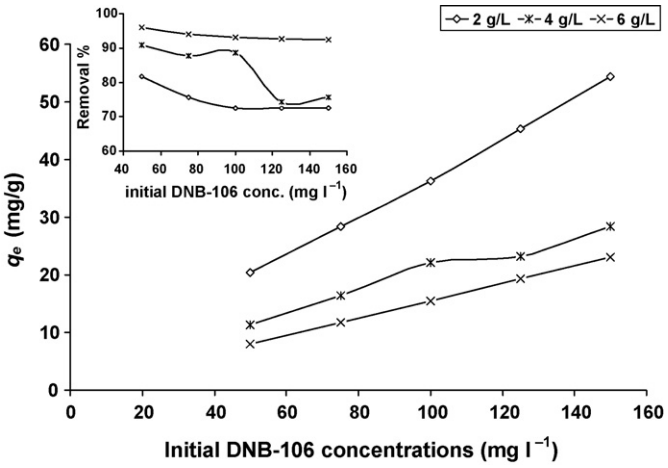

Fig. 6. Inside figure: relation between initial dye concentrations and the removal of DNB-106 (50, 75, 100, 125 and 150 mg l^{-1}) over different COP dose (2, 4 and 6 g l^{-1}) at pH 2.0; main figure: the relation between amounts of dye adsorbed at equilibrium and its initial concentration using different doses of COP.

to 23.09 mg g^{-1} with increasing in the initial dye concentration from 50 to 150 mg l^{-1} using COP doses 2, 4 and 6 g l^{-1}, respectively. The percentage of adsorption efficiency was decreased with the increasing of initial dye concentration in the solution which reflects adsorption decreasing with increasing in initial dye concentration, however, the actual amount of DNB-106 adsorbed per unit mass of adsorbent increased with increasing in DNB-106 concentration.

It is evident from Fig. 6 that the amount of dye adsorbed on the solid phase COP at a lower initial concentration of dye was smaller than the corresponding amount when higher initial concentrations were used. However, the percentage removal of DNB-106 was greater at lower initial concentrations and smaller at higher initial concentrations. In the process of DNB-106 adsorption initially dye molecules have to first encounter the boundary layer effect and then it has to diffuse from boundary layer film onto adsorbent surface and then finally, it has to diffuse into the porous structure of the adsorbent. This phenomenon will take relatively longer contact time. These results clearly indicate that the adsorption of DNB-106 from its aqueous solution was dependent on its initial concentration.

3.5. Effect of adsorbent mass on DNB-106 adsorption

The adsorption of DNB-106 on COP was studied by changing the quantity of adsorbent (0.2, 0.4, 0.6, 0.8 and 1.0 g/100 ml) in the test solution while keeping the initial DNB-106 concentration (150 mg l^{-1}), temperature ($27 \pm 2\,^{\circ}C$) and pH (2.0) constant at different contact times for 3 h (Fig. 7). The percent adsorption was increased and equilibrium time was decreased with adsorbent dose increased. The adsorption increased from 64 to 100%, as the COP dose was increased from 0.2 to 1.0 g/100 ml at equilibrium time (3 h). Maximum DNB-106 removal was achieved within 20 min after which DNB-106 concentration in the reaction solution was almost constant. Increase in the adsorption with adsorbent dose can be attributed to increased COP surface area and availability of more adsorption sites.

3.6. Isotherm data analysis

Adsorption is the accumulation of a mass transfer process that can generally be defined as the material at the interface between solid and liquid phases. Equilibrium relationships between sorbent and sorbate are described by sorption isotherms, usually the ratio

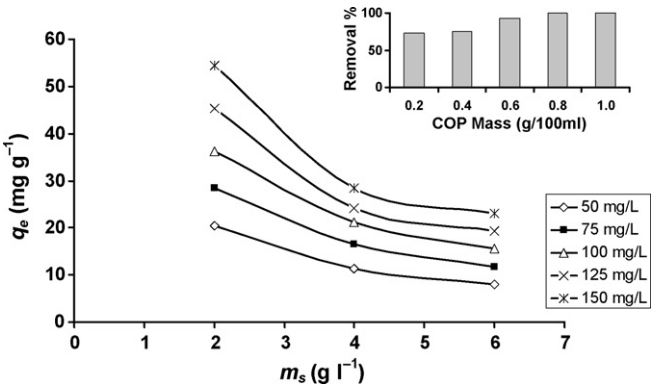

Fig. 7. Inside figure: effect of COP concentration on DNB-106 removals (C_0: 150 mg/l, pH 2.0, agitation speed: 200 rpm and temperature: 27 ± 2 °C); main figure: effect of mass (m_s) of COP concentration on q_e of DNB-106 (C_0: 50–150 mg/l, pH 2.0, agitation speed: 200 rpm and temperature: 27 ± 2 °C).

between the quantity sorbet and that remaining in the solution at a fixed temperature at equilibrium. The adsorption isotherm is important from both a theoretical and a practical point of view. Isotherm data should accurately fit into different isotherm models to find a suitable model that can be used for the design process [28]. The parameters obtained from the different models provide important information on the sorption mechanisms, the surface properties and affinities of the sorbent. There are several isotherm equations available for analyzing experimental sorption equilibrium data, the most famous adsorption models for single-solute systems are the Langmuir and Freundlich models.

The experimental data obtained in the present work was tested with the Langmuir, Freundlich, Redlich–Peterson, Koble–Corrigan, Tempkin, Dubinin–Radushkevich (D–R) and generalized isotherm equations. Linear regression is frequently used to determine the best-fitting isotherm, and the applicability of isotherm equations is compared by judging the correlation coefficients.

3.6.1. Langmuir isotherm

The theoretical Langmuir sorption isotherm [29] is valid for adsorption of a solute from a liquid solution as monolayer adsorption on a surface containing a finite number of identical sites. The model is based on several basic assumptions: (i) the sorption takes place at specific homogenous sites within the adsorbent; (ii) once a dye molecule occupies a site; (iii) the adsorbent has a finite capacity for the adsorbate (at equilibrium); (iv) all sites are identical and energetically equivalent. Langmuir isotherm model assumes uniform energies of adsorption onto the surface without transmigration of adsorbate in the plane of the surface. Therefore, the Langmuir isotherm model was chosen for estimation of the maximum adsorption capacity corresponding to complete monolayer coverage on the sorbent surface. The non-linear equation of Langmuir isotherm model can be written as followed:

$$q_e = \frac{Q_m K_a C_e}{1 + K_a C_e} \tag{2}$$

where C_e and q_e are as defined above in Eq. (1), Q_m is the maximum adsorption capacity reflected a complete monolayer (mg g^{-1}); K_a is adsorption equilibrium constant (l mg^{-1}) that is related to the apparent energy of sorption. The Langmuir isotherm (Eq. (2)) can be linearized into four different forms (Eqs. (3)–(6)), which give different parameter estimates.

Langmuir-1:

$$\frac{C_e}{q_e} = \frac{1}{K_a Q_m} + \frac{1}{Q_m} \times C_e \tag{3}$$

A plot C_e/q_e versus C_e should indicate a straight line of slope $1/Q_m$ and an intercept of $1/(K_a Q_m)$.

Langmuir-2:

$$\frac{1}{q_e} = \left(\frac{1}{K_a Q_m}\right)\frac{1}{C_e} + \frac{1}{Q_m} \tag{4}$$

A plot $1/q_e$ versus $1/C_e$ should have a straight line with a slope of $1/(K_a Q_m)$ and an intercept of $1/Q_m$.

Langmuir-3:

$$q_e = Q_m - \left(\frac{1}{K_a}\right)\frac{q_e}{C_e} \tag{5}$$

A plot q_e versus q_e/C_e should produce a straight line with a slope $1/K_a$ and an intercept of Q_m.

Langmuir-4:

$$\frac{q_e}{C_e} = K_a Q_m - K_a q_e \tag{6}$$

A plot q_e/C_e versus q_e should represent a straight line with slope K_a and an intercept of $K_a Q_m$.

The results obtained from the four forms of Langmuir model for the removal of DNB-106 onto COP are showed in Table 1. The correlation coefficients reported in Table 1 showed strong positive evidence on the adsorption of DNB-106 onto COP follows the Langmuir isotherm. The experimental data obtained was found to be applicable only to the Langmuir-1 form depending on the high correlation coefficients $R^2 > 0.97$, while the other three linear forms of Langmuir model represented lower correlation coefficients (Table 1). Fig. 8 shows the plot of C_e versus q_e obtained from experiments and q_e calculated from Langmuir-1 using 6 g l^{-1} COP concentration and different dye concentration. The maximum monolayer capacity Q_m obtained from Langmuir model was 107.53 mg l^{-1}.

3.6.2. The Freundlich isotherm

The Freundlich isotherm model is the earliest known relationship describing the sorption process [30]. The model applies to adsorption on heterogeneous surfaces with interaction between adsorbed molecules and the application of the Freundlich equation also suggests that sorption energy exponentially decreases on completion of the sorptional centers of an adsorbent. This isotherm is an empirical equation can be employed to describe heterogeneous

Table 1
Isotherm parameters obtained from the four linear forms of Langmuir model for the adsorption of DNB-106 onto activated carbon developed from orange peel.

Model	Orange peel activated carbon concentrations		
	2 g l^{-1}	4 g l^{-1}	6 g l^{-1}
Langmuir-1			
Q_m (mg g^{-1})	107.53	35.59	40.16
$K_a \times 10^{-3}$ (l mg^{-1})	23.38	108.49	112.01
R^2	0.976	0.991	0.981
Langmuir-2			
Q_m (mg g^{-1})	76.34	33.78	30.67
$K_a \times 10^{-3}$ (l mg^{-1})	38.30	112.80	164.90
R^2	0.951	0.948	0.963
Langmuir-3			
Q_m (mg g^{-1})	79.30	31.58	32.91
$K_a \times 10^{-3}$ (l mg^{-1})	36.53	136.77	147.53
R^2	0.644	0.735	0.748
Langmuir-4			
Q_m (mg g^{-1})	102.83	35.64	64.69
$K_a \times 10^{-3}$ (l mg^{-1})	23.50	100.50	47.30
R^2	0.644	0.735	0.932

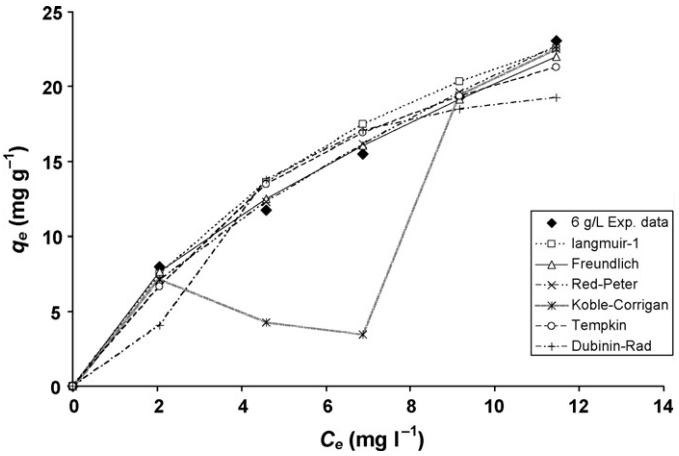

Fig. 8. The plot of C_e versus q_e obtained from experiments and q_e calculated from different isotherm models using 6 g l^{-1} COP concentration and different dye concentration.

systems and is expressed as follow:

$$q_e = K_F C_e^{1/n_F} \quad (7)$$

where K_F is the Freundlich constant (l g^{-1}) related to the bonding energy. K_F can be defined as the adsorption or distribution coefficient and represents the quantity of dye adsorbed onto adsorbent for unit equilibrium concentration. $1/n_F$ is the heterogeneity factor and n_F is a measure of the deviation from linearity of adsorption. Its value indicates the degree of non-linearity between solution concentration and adsorption as follows: if the value of n_F is equal to unity, the adsorption is linear; if the value is below to unity, this implies that adsorption process is chemical; if the value is above to unity adsorption is a favorable physical process [31]. Eq. (7) can be linearized in the logarithmic form (Eq. (8)) and the Freundlich constants can be determined:

$$\log q_e = \log K_F + \frac{1}{n_F} \log C_e \quad (8)$$

The plot of log(q_e) versus log(C_e) was employed to generate the intercept value of K_F and the slope of $1/n_F$ (Table 2). The correlation coefficients, $R^2 > 0.98$, obtained from Freundlich model is comparable to that obtained from Langmuir model linear form 1 (Eq. (3)), while it is much higher than that obtained from the other three linear form of Langmuir model (Fig. 6). This result indicates that the experimental data fitted well to Freundlich model. The values of n_F are higher than unity, indicating that adsorption of DNB-106 onto COP is a favorable physical process [31].

3.6.3. The Redlich–Peterson isotherm

The Redlich–Peterson equation incorporates features of the Langmuir and the Freundlich isotherm models and is represented by non-linear Eq. (9) [32]:

$$q_e = \frac{AC_e}{1 + BC_e^g} \quad (9)$$

where A, B and g are constant and the latter must fluctuate between zero and one. The constant g can characterize the isotherm as: if $g = 1$, the Langmuir will be the preferable isotherm, while if $g = 0$, the Freundlich will be the preferable isotherm. The three isotherm constants A, B and g reported in Table 2 are obtained by solving Eq. (9) using non-linear regression analysis in SPSS program Version 10.0 applicable to computer operation. The correlation coefficient $R^2 > 0.97$ for the two sorbent doses 2 and 6 g l^{-1} with g value 0.293 and 0.39, respectively, while $R^2 = 0.855$ for sorbent dose 4 g l^{-1} with g value 0.753. However Redlich–Peterson isotherm can be consider as less applicability than Langmuir and Freundlich isotherm models for data obtained from adsorption of DNB-86 onto COP (Fig. 8).

Table 2
Comparison of the coefficients isotherm parameters for DNB-106 adsorption onto activated carbon developed from orange peel.

Isotherm model	Orange peel activated carbon concentrations		
	2 g l^{-1}	4 g l^{-1}	6 g l^{-1}
Freundlich			
$1/n_F$	0.636	0.419	0.616
K_F (l g^{-1})	4.73	6.26	4.90
R^2	0.981	0.989	0.986
Koble–Corrigan			
a	3.650	3.940	4.400
b	0.000	0.000	0.000
n	0.716	0.683	0.671
R^2	0.972	0.994	0.990
Redlich–Peterson			
A	52.9	11.3	15.3
B	13.72	0.95	2.60
g	0.293	0.753	0.39
R^2	0.971	0.855	0.988
Tempkin			
A_T	0.245	1.312	1.059
B_T	21.357	6.954	8.523
b_T	116.0	356.3	290.7
R^2	0.905	0.869	0.930
Dubinin–Radushkevich			
Q_m (mg g^{-1})	45.18	24.78	20.70
$K \times 10^{-6}$	13.00	3.40	1.70
E (kJ mol^{-1})	0.196	0.384	0.542
R^2	0.775	0.880	0.958

3.6.4. Koble–Corrigan model

Koble–Corrigan model is another three parameter empirical model depends on the combination of the Langmuir and Freundlich isotherm equations in one non-linear equation for representing the equilibrium adsorption data. It is commonly expressed by Eq. (10) [33]:

$$q_e = \frac{aC_e^n}{1 + bC_e^n} \quad (10)$$

where a, b and n are the Koble-Corrigan parameters, which were also evaluated using SPSS Version 10.0 computer program and reported in Table 2. The correlation coefficients obtained were 0.972, 0.994 and 0.990 for adsorption of DNB-106 onto COP doses 2, 4 and 6 g l^{-1}, respectively, reflected the applicability of Koble–Corrigan model to the experimental data obtained for adsorption of DNB-106 onto COP. However, the value of b was zero for all COP doses tested, which indicates the favorable of Freundlich model over Langmuir model (Fig. 8). This means favorable of heterogeneous adsorption of DNB-106 onto COP at various sorbent doses.

3.6.5. The Tempkin isotherm

Tempkin isotherm model contains a factor that explicitly takes into account adsorbing species–adsorbate interactions [34]. This model assumes the following: (i) the heat of adsorption of all the molecules in the layer decreases linearly with coverage due to adsorbate–adsorbate interactions, and (ii) adsorption is characterized by a uniform distribution of binding energies, up to some maximum binding energy. The derivation of the Tempkin isotherm assumes that the fall in the heat of sorption is linear rather than logarithmic, as implied in the Freundlich equation. The Tempkin isotherm has commonly been applied in the following form (Eq.

(11)) [35]:

$$q_e = \frac{RT}{b_T} \ln(A_T C_e) \quad (11)$$

The Tempkin isotherm (Eq. (11)) can be expressed in its linear form as

$$q_e = B_T \ln A_T + B_T \ln C_e \quad (12)$$

where $B_T = (RT)/b_T$, T is the absolute temperature in Kelvin and R is the universal gas constant, 8.314 J/mol K. The constant b_T is related to the heat of adsorption [36]. The adsorption data were analyzed according to the linear form of the Tempkin isotherm (Eq. (12)). The linear isotherm constants and coefficients of determination are presented in Table 2. Examination of the data shows that the Tempkin isotherm is not applicable to the DNB-106 adsorption onto COP judged by low correlation coefficient (R^2 ranged from 0.869 to 0.930) (Fig. 8).

3.6.6. The Dubinin–Radushkevich (D–R) isotherm

Another equation used in the analysis of isotherms was proposed by Dubinin–Radushkevich [37]. D–R model was applied to estimate the porosity apparent free energy and the characteristic of adsorption [38,39]. The D–R isotherm is dose not assume a homogeneous surface or constant sorption potential and it has commonly been applied in the following form (Eq. (13)) and its linear form can be shown in Eq. (14):

$$q_e = Q_m \exp(-K\varepsilon^2) \quad (13)$$

$$\ln q_e = \ln Q_m - K\varepsilon^2 \quad (14)$$

where K is a constant related to the adsorption energy, Q_m the theoretical saturation capacity, ε is the Polanyi potential can be calculated from Eq. (15):

$$\varepsilon = RT \ln\left(1 + \frac{1}{C_e}\right) \quad (15)$$

The slope of the plot of $\ln q_e$ versus ε^2 gives K (mol^2 (kJ^2)$^{-1}$) and the intercept yields the adsorption capacity, Q_m (mg g^{-1}). The mean free energy of adsorption (E), defined as the free energy change when one mole of ion is transferred from infinity in solution to the surface of the sorbent, was calculated from the K value using the following relation (Eq. (16)) [40]:

$$E = \frac{1}{\sqrt{2K}} \quad (16)$$

Calculated D–R constants for the adsorption of DNB-106 on COP are shown in Table 2; the values of correlation coefficients are much lower than other isotherms values mentioned above. In this case, D–R equation represents the poorer fit of experimental data than the other isotherm equation (Fig. 8). Moreover, the maximum capacity Q_m obtained using D–R isotherm model for adsorption of DNB-106 is 45.18 mg g^{-1} on COP dose of 2 g l^{-1}, which is close to half of that obtained (107.53 mg g^{-1}) from Langmuir-1 isotherm model (Table 1).

3.7. Adsorption dynamics of the adsorption of DNB-106 onto COP

Several steps were used to examine the adsorption dynamics controlling of sorption process such as chemical reaction, diffusion control and mass transfer. Kinetic models are used to test experimental data from the adsorption of DNB-106 onto COP. The kinetics of DNB-106 adsorption onto COP is required for selecting optimum operating conditions for the full-scale batch process. The kinetic parameters, which are helpful for the prediction of adsorption rate, give important information for designing and modeling the adsorption processes. Thus, pseudo-first-order [41], pseudo-second-order [42], Elovich [43–45] and intraparticle diffusion [46,47] kinetic models were used for the adsorption of DNB-106 onto COP. The conformity between experimental data and the model-predicted values was expressed by the correlation coefficients (R^2, values close or equal to 1, the relatively higher value is the more applicable model).

3.7.1. Pseudo-first-order equation

The adsorption kinetic data were described by the Lagergren pseudo-first-order model [41], which is the earliest known equation describing the adsorption rate based on the adsorption capacity. The Lagergren equation is commonly expresses as follows:

$$\frac{dq_t}{dt} = k_1(q_e - q_t) \quad (17)$$

where q_e and q_t are the adsorption capacity at equilibrium and at time t, respectively (mg g^{-1}), k_1 is the rate constant of pseudo-first-order adsorption (l min^{-1}). Integrating Eq. (17) for the boundary conditions $t = 0$ to $t = t$ and $q_t = 0$ to $q_t = q_t$ gives:

$$\log\left(\frac{q_e}{q_e - q_t}\right) = \frac{k_1}{2.303} t \quad (18)$$

Eq. (18) can be rearranged to obtain the following linear form:

$$\log(q_e - q_t) = \log(q_e) - \frac{k_1}{2.303} t \quad (19)$$

Plot the values of $\log(q_e - q_t)$ versus t to give a linear relationship from which k_1 and q_e can be determined from the slope and intercept, respectively (Fig. 9). If the intercept dose not equal q_e then the reaction is not likely to be first-order reaction even this plot has high correlation coefficient with the experimental data [31]. The variation in rate should be proportional to the first power of concentration for strict surface adsorption. However, the relationship between initial solute concentration and rate of adsorption will not be linear when pore diffusion limits the adsorption process. Fig. 9 shows that the first 30 min data fits well Lagergren model and thereafter the adsorption data deviate from theory. Thus, the model represents the initial stages where rapid adsorption occurs well but cannot be applied for the entire adsorption process. Furthermore, the calculated q_e values are too low compared with experimental q_e values and the correlation coefficient R^2 are relatively low for most adsorption data (Table 3), which indicates that the adsorption of DNB-106 onto COP are not a first-order reaction.

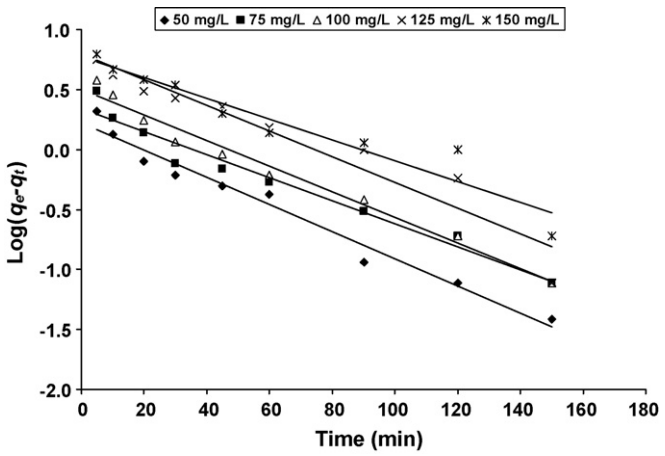

Fig. 9. Pseudo-first-order kinetics for DNB-106 (50, 75, 100, 125 and 150 mg l^{-1}) adsorption onto COP. Conditions: adsorbent dosage 6 g l^{-1}, pH 2.0 and temperature 27 ± 2 °C.

Table 3
Comparison of the first- and second-order adsorption rate constants and calculated and experimental q_e values for different initial DNB-106 and activated carbon developed from orange peel.

Parameter			First-order kinetic model			Second-order kinetic model			
Carbon conc.	DNB-106 ($mg\,l^{-1}$)	q_e (exp.)	$k_1 \times 10^{-3}$	q_e (calc.)	R^2	$k_2 \times 10^{-3}$	q_e (calc.)	h	R^2
	50	20.42	8.98	5.46	0.925	7.063	20.20	2.88	0.993
	75	28.34	19.58	7.79	0.901	6.111	28.90	5.10	0.997
$2\,g\,l^{-1}$	100	36.26	18.65	9.45	0.985	6.074	36.76	8.21	1.000
	125	45.33	30.86	10.3	0.964	7.707	46.08	16.37	1.000
	150	54.39	14.97	10.97	0.964	4.819	54.64	14.39	0.999
	50	11.36	23.03	4.74	0.933	11.537	11.67	1.57	0.997
	75	16.46	13.13	4.19	0.936	11.669	16.50	3.18	0.998
$4\,g\,l^{-1}$	100	22.14	15.20	5.7	0.894	9.386	22.27	4.66	0.999
	125	23.24	20.27	6.05	0.970	9.619	23.58	5.35	0.999
	150	28.34	18.19	8.71	0.781	6.354	28.49	5.16	0.997
	50	7.99	26.02	1.25	0.973	45.225	8.09	2.96	1.000
	75	11.74	22.11	2.20	0.960	31.758	11.85	4.46	1.000
$6\,g\,l^{-1}$	100	15.52	24.64	3.15	0.979	23.536	15.70	5.80	1.000
	125	19.31	24.64	6.24	0.923	10.858	19.65	4.19	0.999
	150	23.09	20.04	5.95	0.920	10.280	23.36	5.61	0.999

3.7.2. Pseudo-second-order equation

The adsorption kinetic may be described by the pseudo-second-order model [42], which is generally given as following:

$$\frac{dq_t}{dt} = k_2(q_e - q_t)^2 \tag{20}$$

where k_2 ($g\,mg^{-1}\,min^{-1}$) is the second-order rate constant of adsorption. Integrating Eq. (20) for the boundary conditions $q_t = 0$ to $q_t = q_t$ at $t = 0$ to $t = t$ is simplified as can be rearranged and linearized to obtain:

$$\left(\frac{t}{q_t}\right) = \frac{1}{k_2 {q_e}^2} + \frac{1}{q_e}(t) \tag{21}$$

The second-order rate constants were used to calculate the initial sorption rate, given by the following Eq. (22):

$$h = k_2 q_e^2 \tag{22}$$

It was mentioned above that the curve fitting plots of $\log(q_e - q_t)$ versus t does not show good results for the entire sorption period, while the plots of t/q_t versus t give a straight line for all the initial dye concentrations studied as showed in Fig. 10, confirming the applicability of the pseudo-second-order equation. Values of k_2 and equilibrium adsorption capacity q_e were calculated from the intercept and slope of the plots of t/q_t versus t, respectively. The values of R^2 and q_e also indicated that this equation produced better results (Table 3): at all concentrations and sorbent doses, R^2 values for pseudo-second-order kinetic model were found to be higher (between 0.993 and 1.000), and the calculated q_e values are mainly equal to the experimental data. This indicates that the DNB-106-COP adsorption system obeys the pseudo-second-order kinetic model for the entire sorption period.

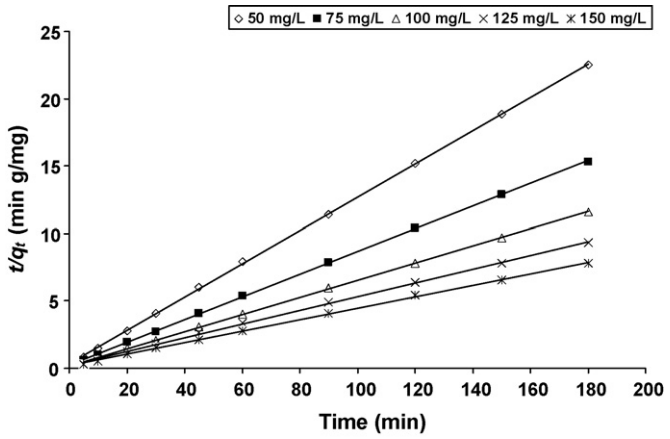

Fig. 10. Plot of the pseudo-second-order model at different initial DNB-106 concentrations (50, 75, 100, 125 and $150\,mg\,l^{-1}$), COP $6\,g\,l^{-1}$, pH 2.0 and temperature $27 \pm 2\,^{\circ}C$.

The values of initial sorption (h, $mg\,g^{-1}\,min^{-1}$) that represents the rate of initial sorption, is practically increased with the increase in initial dye concentrations from 50 to $150\,mg\,l^{-1}$ onto COP dose 2.0, 4.0 and $5.0\,g\,l^{-1}$, respectively (Table 3). It was observed that the pseudo-second-order rate constant (k_2) decreased with increasing of initial dye concentration from 50 to $150\,mg\,l^{-1}$ for COP doses of 2, 4 and $6\,g\,l^{-1}$, respectively.

3.7.3. Elovich kinetic equation

The Elovich equation is another rate equation based on the adsorption capacity is given as follows [43–45]:

$$\frac{dq_t}{dt} = \alpha \exp(-\beta q_t) \tag{23}$$

where α is the initial adsorption rate ($mg\,g^{-1}\,min^{-1}$) and β is the de-sorption constant ($g\,mg^{-1}$) during any one experiment.

It is simplified by assuming $\alpha\beta \gg t$ and by applying the boundary conditions $q_t = 0$ at $t = 0$ and $q_t = q_t$ at $t = t$ Eq. (23) rewrite as followed:

$$q_t = \frac{1}{\beta}\ln(\alpha\beta) + \frac{1}{\beta}\ln(t) \tag{24}$$

Plot of q_t versus $\ln(t)$ should yield a linear relationship if the Elovich is applicable with a slope of $(1/\beta)$ and an intercept of $(1/\beta)\ln(\alpha\beta)$ (Fig. 11). The Elovich constants obtained from the slope and the intercept of the straight line reported in Table 4. The correlation coefficients R^2 are very wavy and ranged from low value to high value without definite role (Table 4).

3.7.4. The intraparticle diffusion model

Adsorption is a multi-step process involving transport of the adsorbate (dye) molecules from the aqueous phase to the surface of the solid (COP) particles then followed by diffusion of the solute molecules into the pore interiors. If the experiment is a batch system with rapid stirring, there is a possibility that the transport of sorbate from solution into pores (bulk) of the adsorbent is the rate-controlling step [48]. This possibility was tested in terms of a graphical relationship between the amount of dye adsorbed and the square root of time [46]. Since the DNB-106 is probably transported

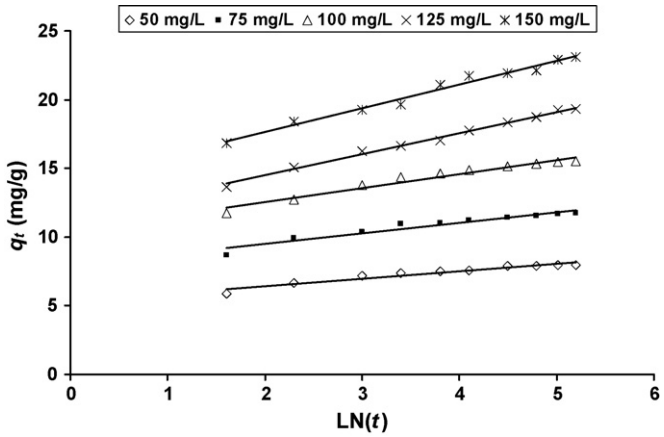

Fig. 11. Elovich model plot for the adsorption of DNB-106 (50, 75, 100, 125 and 150 mg l^{-1}) onto COP (6.0 g l^{-1}) at different initial dye concentrations (50, 75, 100, 125 and 150 mg l^{-1}).

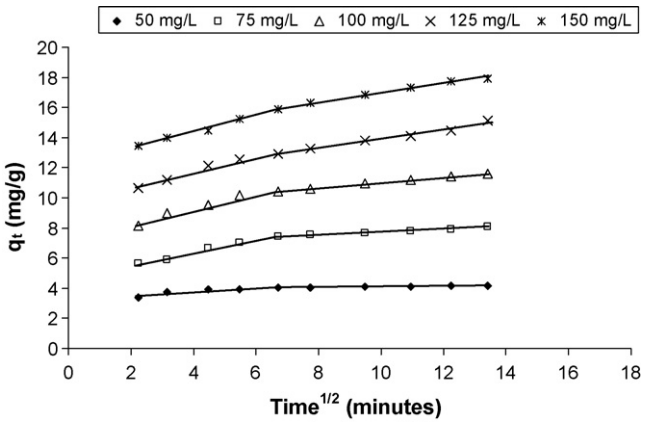

Fig. 12. Intraparticle diffusion model plot for the adsorption of DNB-106 (50, 75, 100, 125 and 150 mg l^{-1}) onto COP (6.0 g l^{-1}) at different initial dye concentration (50, 75, 100, 125 and 150 mg l^{-1}) and room temperature.

from its aqueous solution to the COP by intraparticle diffusion, so the intraparticle diffusion is another kinetic model should be used to study the rate-limiting step for DNB-106 adsorption onto COP. The intra-particular diffusion is commonly expressed by the following equation:

$$q_t = K_{dif} t^{1/2} + C \quad (25)$$

where C is the intercept and K_{dif} (in mg g^{-1} $min^{-1/2}$) is the intra-particle diffusion rate constant. The values of q_t were found to give two lines part with values of $t^{1/2}$ (Fig. 12) and the rate constant K_{dif} directly evaluated from the slope of the second regression line and the values of intercept C, which is related to the thickness of the boundary layer was reported in Table 4. The shape of Fig. 12 confirms that adsorption of the DNB-106 onto the COP is independent of one another, as plot usually shows two intersecting lines depending on the exact mechanism; the first one of these lines representing surface adsorption at the beginning of the reaction and the second one is the intraparticle diffusion at the end of the reaction. As still there is no sufficient indication about which of the two steps is the rate-limiting step. Ho [49] has shown that if the intraparticle diffusion is the sole rate-limiting step, it is essential for the q_t versus $t^{1/2}$ plots to pass through the origin, which is not the case in Figs. 12, it may be concluded that surface adsorption and intraparticle diffusion were concurrently operating during the DNB-106-COP interactions.

Fig. 13 represents the plot between the values of intercept C versus different initial dye concentration for three different COP doses. The constant C was found to increase with increase of dye concentration from which indicating the increase of the thickness of the boundary layer and decrease of the chance of the external mass transfer and hence increase of the chance of internal mass transfer. On the other hand, the constant C was found to decrease with the increase of COP dose, which reflect decrease of the thickness of the boundary layer and hence increase of the chance of the external mass transfer. The R^2 values given in Table 4 are close to unity indicating the application of this model, which may confirm that the rate-limiting step is the intraparticle diffusion process. The intraparticle diffusion rate constant, K_{dif}, were in the range of 0.02–0.80 mg g^{-1} $min^{-1/2}$ and it decrease with increase of initial dye concentration and increase of COP dose.

Table 4
The parameters obtained from Elovich kinetics model and intraparticle diffusion model using different initial DNB-106 concentrations.

Sorbent dose	DNB-106 (mg l^{-1})	Elovich			Intraparticle diffusion		
		β	$\alpha \times 10^3$	R^2	K_{dif}	C	R^2
2 g l^{-1}	50	0.85	66.80	0.737	0.50	13.10	1.000
	75	0.64	372.1	0.735	0.59	21.02	0.969
	100	0.35	5.32	0.977	0.51	29.51	0.993
	125	0.33	85.50	0.916	0.60	39.24	0.978
	150	0.32	454.3	0.962	0.80	43.51	0.997
4 g l^{-1}	50	0.95	0.24	0.942	0.06	5.54	0.989
	75	0.81	3.08	0.959	0.21	7.30	0.972
	100	0.51	0.88	0.965	0.16	10.15	0.969
	125	0.58	7.33	0.970	0.31	12.61	0.988
	150	0.48	6.32	0.954	0.43	15.33	0.992
6 g l^{-1}	50	1.83	9.64	0.938	0.02	3.94	0.979
	75	1.29	21.49	0.930	0.09	6.80	0.969
	100	0.97	26.15	0.960	0.18	9.21	0.998
	125	0.65	1.37	0.993	0.31	10.86	0.982
	150	0.58	6.77	0.981	0.31	13.90	0.994

3.8. Simulation DNB-106 wastewater

It is well known that the textile wastewater dose not has only dye but it also contains some other additive such as Na_2SO_4, NaCl, Na_2CO_3, HCOOH and CH_3COOH depending on the type of dye, dyeing method and required color degree, therefore a simulated wastewater according to ISMA dyeing catalog were prepared as

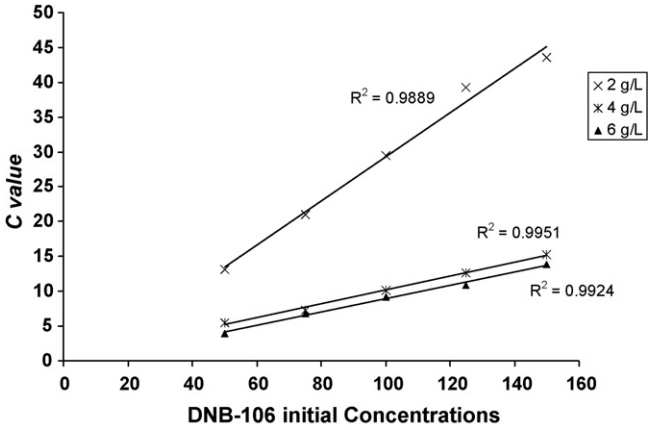

Fig. 13. Plot of DNB-106 initial concentrations (50, 75, 100, 125 and 150 mg l^{-1}) versus intraparticle diffusion constant C value obtained for different COP doses at room temperature.

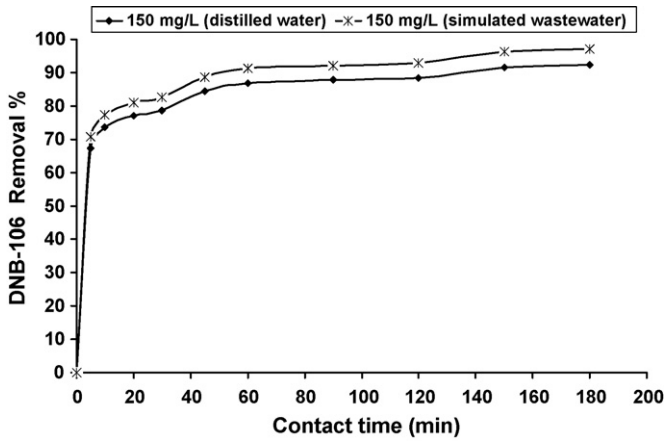

Fig. 14. Effect of dyeing additive on the removal of DNB-106 using COP, dye concentration (150 mg l^{-1}), COP dose (6.0 g l^{-1}) and room temperature.

mentioned above in materials and methods and used instead of solution in distilled water. The results obtained are represented by Fig. 14, which shows enhanced of the percentage of dye removal from 92 to 97% using 150 mg l^{-1} initial dye concentration over 6 g l^{-1} sorbent dose. These results indicate that the COP is applicable sorbent for removal of direct dyes (DNB-106) from the dyeing waste.

4. Conclusion

The results of this work can be summarized as follows: (i) activated carbon developed from orange peel is a promising adsorbent for removal of the anionic dye, DNB-106 from wastewater. A small amount (2 g l^{-1}) of COP could almost remove over 75% of 150 mg l^{-1} of DNB-106 within 3 h contact time; (ii) the solution pH has important bearing on the extent of adsorption of the dye on COP, which indicating that the pH is more important in the controlling of adsorption rather than the nature of the surface sites. This result was also proved by Koble–Corrigan isotherm model, which fitted well the data with constant *b* value equal zero that confirm Freundlich isotherm model; (iii) the experimental data showed perfect fit with the Freundlich isotherm, which confirm that the adsorption process is heterogeneous, non-specific and non-uniform in nature. Therefore, the mechanism of DNB-106-COP interactions is complicated involving a wide range of sites differing in a number of aspects including energy considerations. On the other hand, the data obtained were in good agreement with the Langmuir-1; (iv) moreover, the data did not agree with Redlich–Peterson, Tempkin and Dubinin–Radushkevich isotherm models; (v) the kinetic study of DNB-106 on COP was investigated using pseudo-first-order, pseudo-second-order, Elovich and intraparticle diffusion equations. The results indicate that the adsorption kinetics follow the pseudo-second-order rate with intraparticle diffusion as one of the rate determining steps. This work confirms that the COP could be used for the removal of direct dyes from wastewater.

References

[1] V.A. Shenai, Azo dyes on textiles vs. German ban: an objective assessment. Part III. Another study, Colourage XLIII (8) (1996) 41.
[2] J.C. Greene, G.L. Baughman, Effects of 46 dyes on population growth of fresh green algae *Selenastrum capricornutum*, Text. Chem. Color. 28 (4) (1996) 23.
[3] C. Saha, Eco-textile: a novel concept of cleaner product, Text Dyer Printer XXIX (21) (1996) 13.
[4] D.A.S. Phillips, Environmentally friendly, productive and reliable priorities for cotton dyes and dyeing processes, J. Soc. Dyers Color. 112 (1996) 183.
[5] M.F. Boeniger, Carcinogenity of Azo Dyes Derived from Benzidine, Department of Health and Human Services (NIOSH), Pub. No. 8-119, Cincinnati, OH, 1980.
[6] Kirk-Othmer, Encyclopedia of Chemical Technology, Explosives and Propellants to Flame Retardants for Textiles, 4th ed., Wiley-Interscience Publishers, 1994, pp. 547–672, ISBN-13: 978-0471526780.
[7] M.C. Yu, P.L. Skipper, S.R. Tannenbaum, K.K. Chan, P.K. Ross, Arylamine exposures and bladder cancer risk, Mutat. Res. Fundam. Mol. Mech. Mutagen. 506/507 (2002) 21–28.
[8] T. Zheng, T.R. Holford, S.T. Mayne, P.H. Owens, P. Boyle, B. Zhang, et al., Use of hair coloring products and breast cancer risk: a case-control study in Connecticut, Eur. J. Cancer 38 (2002) 1647–1652.
[9] K.R. Ramakrishna, T. Viraraghavan, Dye removal using low cost adsorbent, Water Sci. Technol. 36 (1997) 189–196.
[10] A. Bozdogan, H. Goknil, The removal of the color of textile dyes in wastewater by the use of recycled coagulant, MU Fen. Billimeri. Dergisi. Sayi. 4 (1987) 83.
[11] K. Majewska-Nowak, Effect of flow conditions on ultrafiltration efficiency of dye solutions and textile effluents, Desalination 71 (1989) 127.
[12] O.R. Shendrik, Electro membrane removal of organic dyes from wastewaters, Kimiyi. Technol. Vody. 11 (1989) 467.
[13] Z. Ding, C.W. Min, W.Q. Hui, A study on the use of bipolar particles-electrode in the decolorization of dying effluents and its principle, Water Sci. Technol. 19 (3/4) (1987) 39.
[14] O. Abdelwahab, A. El Nemr, A. El-Sikaily, A. Khaled, Biosorption of Direct Yellow 12 from aqueous solution by marine green algae *Ulva Lactuca*, Chem. Ecol. 22 (2006) 253–266.
[15] A. El-Sikaily, A. Khaled, A. El Nemr, O. Abdelwahab, Removal of methylene blue from aqueous solution by marine green alga *Ulva lactuca*, Chem. Ecol. 22 (2006) 149–157.
[16] Y.S. Ho, T.H. Chiang, Y.M. Hsueh, Removal of basic dye from aqueous solution using tree fern as a biosorbent, Process Biochem. 40 (2005) 119–124.
[17] M. Özacar, İ.A. Şengil, A kinetic study of metal complex dye sorption onto pine sawdust, Process Biochem. 40 (2005) 565–572.
[18] G. Akkaya, İ. Üzun, F. Guzel, Kinetics of the adsorption of reactive dyes by chitin, Dyes Pigments 73 (2007) 168–177.
[19] P. Cooper, Color in Dye House Effluent. Soc Dyers and Colorists, Alden Press, Oxford, 1995.
[20] J.W. Hassler, Activated Carbon, Chem. Publ., New York, 1963.
[21] K. Kannan, M.M. Sndaram, Kinetics and mechanism of removal of methylene blue by adsorption on various carbons—a comparative study, Dyes Pigments 51 (2001) 25–40.
[22] R. Sivaraj, C. Namasivayam, K. Kadirvelu, Orange peel as an adsorbent in the removal of Acid violet 17 (acid dye) from aqueous solutions, Waste Manage. 21 (2001) 105–110.
[23] M. Arami, N.Y. Limaee, N.M. Mahmoodi, N.S. Tabrizi, Removal of dyes from colored textile wastewater by orange peel adsorbent: equilibrium and kinetic studies, J. Colloid Interface Sci. 288 (2005) 371–376.
[24] F.D. Ardejani, K.H. Badii, N.Y. Limaee, N.M. mahmoodi, M. Arami, S.Z. Shafaei, A.R. Mirhabibi, Numerical modeling and laboratory studies on the removal of Direct Red 23 and Direct Red 80 dyes from textile effluents using orange peel, a low-cost adsorbent, Dye Pigments 73 (2007) 178–185.
[25] C. Namasivayam, D. Kavitha, Removal of Congo Red from water by adsorption onto activated carbon prepared from coir pith, an agricultural solid waste, Dyes Pigments 54 (1) (2002) 47–58.
[26] C. Namasivayam, R. Radhika, S. Suba, Uptake of dyes by promising locally available agricultural solid wastes coir pith, Waste Manage. 21 (4) (2001) 381–387.
[27] P.K. Malik, Dye removal from wastewater using activated carbon developed from sawdust: adsorption equilibrium and kinetics, J. Hazard. Mater. B 113 (2004) 81–88.
[28] E.R. Alley, Water Quality Control Handbook, McGraw-Hill Education Publishers, 2000, pp. 125–141, ISBN0070014132 / 9780070014138 / 0-07-001413-2 http://www.bookfinder.com/author/e-roberts-alley/.
[29] I. Langmuir, The constitution and fundamental properties of solids and liquids, J. Am. Chem. Soc. 38 (1916) 2221–2295.
[30] H.M.F. Freundlich, Über die adsorption in lösungen, Z. Phys. Chem. (Leipzig) 57A (1906) 385–470.
[31] G. Crini, H.N. Peindy, F. Gimbert, C. Robert, Removal of C.I. Basic Green 4 (Malachite Green) from aqueous solutions by adsorption using cyclodextrin based adsorbent: kinetic and equilibrium studies, Sep. Purif. Technol. 53 (2007) 97–110.
[32] O. Redlich, D.L. Peterson, A useful adsorption isotherm, J. Phys. Chem. 63 (1959) 1024.
[33] R.A. Koble, T.E. Corrigan, Adsorption isotherm for pure hydrocarbons, Ind. Eng. Chem. 44 (1952) 383–387.
[34] M.J. Tempkin, V. Pyzhev, Acta Physiochim. URSS 12 (1940) 217–222.
[35] C. Aharoni, D.L. Sparks, Kinetics of soil chemical reactions—a theoretical treatment, in: D.L. Sparks, D.L. Suarez (Eds.), Rate of Soil Chemical Processes, Soil Science Society of America, Madison, WI, 1991, pp. 1–18.
[36] G. Akkaya, A. Ozer, Adsorption of acid red 274 (AR 274) on Dicranella varia: determination of equilibrium and kinetic model parameters, Process Biochem. 40 (11) (2005) 3559–3568.
[37] C.I. Pearce, J.R. Lioyd, J.T. Guthrie, The removal of color from textile wastewater using whole bacterial cells: a review, Dyes Pigments 58 (2003) 179–196.
[38] M.M. Dubinin, Modern state of the theory of volume filling of micropore adsorbents during adsorption of gases and steams on carbon adsorbents, Zh. Fiz. Khim. 39 (1965) 1305–1317.

[39] L.V. Radushkevich, Potential theory of sorption and structure of carbons, Zh. Fiz. Khim. 23 (1949) 1410–1420.
[40] S. Kundu, A.K. Gupta, Investigation on the adsorption efficiency of iron oxide coated cement (IOCC) towards As (V)-Kinetics, equilibrium and thermodynamic studies, Colloids Surf. A: Physicochem. Eng. Aspects 273 (2006) 121–128.
[41] S. Lagergren, Zur theorie der sogenannten adsorption geloster stoffe. Kungliga Svenska Vetenskapsakademiens, Handlingar 24 (1898) 1–39.
[42] Y.S. Ho, G. McKay, D.A.J. Wase, C.F. Foster, Study of the sorption of divalent metal ions on to peat, Adsorpt. Sci. Technol. 18 (2000) 639–650.
[43] S.H. Chien, W.R. Clayton, Application of Elovich equation to the kinetics of phosphate release and sorption on soils, Soil Sci. Soc. Am. J. 44 (1980) 265–268.
[44] D.L. Sparks, Kinetics of reaction in pure and mixed systems, in: Soil Physical Chemistry, CRC Press, Boca Raton, 1986.
[45] J. Zeldowitsch, Über den mechanismus der katalytischen oxidation von CO an MnO_2, Acta Physiochim. URSS 1 (1934) 364–449.
[46] W.J. Weber, J.C. Morris, Kinetics of adsorption on carbon from solution, J. Sanity Eng. Div. Am. Soc. Civil Eng. 89 (1963) 31–59.
[47] K. Srinivasan, N. Balasubramanian, T.V. Ramakrishan, Studies on chromium removal by rice husk carbon, Indian J. Environ. Health 30 (1988) 376–387.
[48] G. McKay, The adsorption of dyestuff from aqueous solution using activated carbon: analytical solution for batch adsorption based on external mass transfer and pore diffusion, Chem. Eng. J. 27 (1983) 187–195.
[49] Y.S. Ho, Removal of copper ions from aqueous solution by tree fern, Water Res. 37 (2003) 2323–2330.